


RESEARCH

Open Access



# Regeneration of beaded activated carbon saturated with volatile organic compounds by a novel electrothermal swing adsorption system

Hao-Chih Yu<sup>1</sup>, Shu-Wen You<sup>1</sup>, Can Wang<sup>2,3</sup>, Ji-Guang Deng<sup>4</sup> and Hsing-Cheng Hsi<sup>1\*</sup> 

## Abstract

A commercially available beaded activated carbon (KBAC) was selected for combination with a novel electrothermal swing system in examining the Joule heating effects on the physical and chemical properties of activated carbon and its adsorption regenerability at various regeneration temperatures (120, 140, and 160 °C) after saturation by toluene (TOL) and methylethylketone (MEK). The specific surface area ( $1278 \text{ m}^2 \text{ g}^{-1}$ ) and micropore volume ( $0.48 \text{ cm}^3 \text{ g}^{-1}$ ) for KBAC after one adsorption/desorption cycle were slightly reduced, while KBAC micropore surface area ( $1158 \text{ m}^2 \text{ g}^{-1}$ ) and micropore volume decreased significantly after six adsorption/desorption cycles. It can be inferred that the pores of KBAC, especially micropores, are blocked by heel buildup caused mainly by formation of cracked TOL and MEK coke generated by cyclic Joule heating. The desorption efficiencies of TOL-KBAC and MEK-KBAC (KBAC saturated with TOL and MEK, respectively) evaluated per the gravimetric method ranged from 55 to 80 and 85–90%, respectively, and both showed great correlation between regeneration temperature and desorption efficiency. Notably, the desorption efficiencies calculated from the integral method based on breakthrough curves were 8 and 16% lower than those directly obtained by the gravitational method for TOL-KBAC and MEK-KBAC, respectively. The larger difference in desorption efficiency evaluated by the two methods for MEK-KBAC is likely caused by the decomposition of MEK into CO or  $\text{CO}_2$ , which was less prominent in TOL-KBAC. In the cyclic adsorption/desorption tests, the adsorption capacities of both TOL-KBAC and MEK-KBAC decreased after the 6-cycle electrothermal swing regeneration, such that TOL-KBAC adsorption capacity significantly reduced to around 50%, while that of MEK-KBAC retained around 70% of their respective original adsorption capacities. As aforementioned, heel buildup blocks the pores and leads to decreasing adsorption, especially for TOL.

**Keywords:** Beaded activated carbon, Volatile organic compounds, Toluene, Methylethylketone, Electrothermal swing regeneration

## 1 Introduction

Volatile organic compounds (VOCs) are common air pollutants emitted from anthropogenic activities and are harmful to human beings and the earth's environment. In addition to the profound adverse effects on human health, VOCs indirectly enhance global warming effects as they undergo complex, long-term transport photochemical reactions in the stratosphere. Since VOCs are

\*Correspondence: hchsi@ntu.edu.tw

<sup>1</sup> Graduate Institute of Environmental Engineering, National Taiwan University, Taipei 10617, Taiwan  
Full list of author information is available at the end of the article



© The Author(s) 2022. **Open Access** This article is licensed under a Creative Commons Attribution 4.0 International License, which permits use, sharing, adaptation, distribution and reproduction in any medium or format, as long as you give appropriate credit to the original author(s) and the source, provide a link to the Creative Commons licence, and indicate if changes were made. The images or other third party material in this article are included in the article's Creative Commons licence, unless indicated otherwise in a credit line to the material. If material is not included in the article's Creative Commons licence and your intended use is not permitted by statutory regulation or exceeds the permitted use, you will need to obtain permission directly from the copyright holder. To view a copy of this licence, visit <http://creativecommons.org/licenses/by/4.0/>.

released from various sources in significant amounts, the Taiwanese government has relentlessly tried to clarify the distribution of VOCs to form appropriate strategies for VOCs abatement. Therefore, it is imperative to reduce VOCs emission from stationary sources and explore relatively sustainable recycling techniques in the reuse of high-priced VOCs [1–4].

Myriad control techniques, including absorption, thermal/catalytic oxidation, biotreatment, and adsorption, have been developed in response to necessary VOCs release reduction in the environment. An adsorption-based process combined with a suitable adsorbent has been regarded as one of the most promising strategies to remove low concentrations of VOCs due to its high removal efficiency, simplicity, cost-effectiveness, and low energy requirement [1, 5–11]. Among commonly used adsorbents, activated carbon (AC) is a compelling material per the following advantages: high surface area and pore volume, low cost, accessibility, reusability, and ease of tailoring. In addition, employing adsorption via AC is economically feasible for recovering valuable solvents by adsorbent regeneration, which is equally significant to the adsorption process [12–14].

One widely used AC for VOC capture is beaded AC (BAC), which could be produced from various polymeric precursors, including divinylbenzene-based polymer [15], copolymer of vinylidene chloride and styrene [16], polystyrene-based resin [17], and phenol-formaldehyde (PF) resin [18, 19]). Its outstanding characteristics, including high abrasive resistance, low ash content, good fluidity, low pressure drops, porous structure, and excellent adsorption performance, have enabled it to be adopted en masse in various industrial applications [1, 18, 20, 21]. We have compared a self-prepared BAC (SBAC) derived from waste bamboo tar or PF resins with a commercially available KBAC (where K stands for Kureha Corp., Japan) based on their physical properties, and adsorption performance toward toluene (TOL) and methylethylketone (MEK). Detailed information regarding the comparison of these BACs may be found in our previous studies [22–24]. Briefly, the adsorption capacities of TOL on the BACs could be up to 85% greater than those of MEK under the same test conditions, suggesting a stronger nonpolar interaction between TOL molecules and the adsorbent [23]. Hsiao et al. [24] also showed that physisorption is the dominant TOL and MEK adsorption mechanisms by the two tested BACs, and the adsorption amount influences the adsorption heat.

After amassing VOC on the adsorbent, it is necessary to desorb the adsorbate, a reverse behavior of the adsorption process, to limit the replacement frequency of AC, operating costs, and potential environmental damage due to incineration or landfilling of toxic pollutant-laden

AC. The hot steam method is conventionally adopted for AC regeneration. Nevertheless, a tremendous amount of energy is required for the regeneration process, and separating VOCs from the effluent gas stream is tedious. Furthermore, water vapor condensation within the pore structure of AC worsens adsorption performance due to stronger competition with the water molecules, thereby either increasing the cost of replacement AC or waiting time between operating procedures. Our earlier works [23, 24] have shown that microwave regeneration is effective and feasible in regenerating BAC samples within a short period. Additionally, an electrothermal swing system (ETS) has also been shown to successfully overcome the abovementioned defects of conventional hot steam regeneration [25–31]; the ETS has been applied for continuous adsorption and desorption of gaseous pollutants such as CO<sub>2</sub>, VOCs, and even elemental mercury.

Compared with conventional thermal treatments (e.g., hot steam and furnace heating), ETS is a promising and competitive technique per the merits highlighted below [28]:

1. High energy efficiency: Whereas conventional thermal treatment requires massive energy input to raise the temperature of the water or inert gas for adsorbent regeneration, ETS applies current directly to the adsorbent, and the Joule effect occurs due to the adsorbent's conductivity, while heterogeneous distributed resistivity raises the adsorbent's temperature despite low energy input. More importantly, the entire electrothermal regeneration process takes only a few minutes to complete [30], while the hot steam method or furnace heating requires 0.5–20 h.
2. High flexibility: The heat capacity of the carrier gas is unrelated to the heating of the adsorbent. Namely, there is no limitation in the ratio of gas volume to mass of adsorbent for heat transfer. Therefore, the outlet concentrations can be easily controlled by adjusting the flow rate of the carrier gas.
3. Simplicity: The setup and operation of an ETS are much simpler and eco-friendlier than the hot steam regeneration method. Notably, an electrothermal regeneration process does not generate wastewater and subsequent treatment of regenerated adsorbents is unnecessary.

Adsorbents such as AC monolith and AC fiber cloth are commonly selected for ETS adsorption and regeneration due to their appropriate morphologies and physical properties, including heterogeneous distributed resistivity and conductivity, which lead to the Joule effect heating up the adsorbent directly. Nevertheless, to our best knowledge, there is still little research regarding VOC adsorption and regeneration using BAC combined

with an ETS. This study concentrates on investigating the feasibility of KBAC regeneration using a novel ETS after saturation with TOL and MEK, two major solvents emitted from the polyurethane industry in Taiwan. The main objectives of the present research are: (i) characterizing the physicochemical properties of KBAC before and after electrothermal regeneration, (ii) exploring the effect of regeneration temperatures (120, 140, and 160 °C) on the regenerated KBAC, and (iii) identifying the heel buildup effect during a consecutive cyclic adsorption/regeneration experiment, and subsequently proving the feasibility of this technology. The findings from this study can help develop a new pathway for effective VOC adsorption/recovery and adsorbent regeneration approaches when BACs are applied in a joint fluidized-bed adsorption/ETS system.

## 2 Materials and methods

### 2.1 Adsorbent preparation and characterization

KBAC was commercially obtained, dried in an oven at 105 °C for 24 h to remove adsorbed moisture, and placed in a desiccator prior to experiments.

The chemical composition of KBAC was analyzed by an elemental analyzer (Elementar, model vario EL cube). The sample was completely burned and the mass fraction of each element, C, H, O, N, and S, was determined based on the gas mixture by a thermal conductivity detector downstream.

The surface morphology of virgin and regenerated KBAC was analyzed using a scanning electron microscopy (SEM, JEOL model JSM-7600F) with an accelerating voltage of 10 kV. The N<sub>2</sub> adsorption was carried out at 77 K using Micromeritics model ASAP 2420 instrument.

All samples were degassed at 150 °C for 15 h to remove moisture and impurities prior to analyses. The total specific surface area ( $S_{total}$ ) was obtained based on the Brunauer-Emmett-Teller equation. Total pore volume ( $V_{total}$ ) was calculated using the Barret-Joyner-Halenda method and recorded at  $P/P_0=0.994$ . Micropore surface area ( $S_{micro}$ ) and micropore volume ( $V_{micro}$ ) were obtained from the t-plot analysis by applying the Harkins and Jura thickness curve,  $t=[13.99/(0.034-\log(P/P_0))]^{0.5}$ . The range of relative pressures used to determine  $S_{micro}$  and  $V_{micro}$  was based on a statistical thickness t-value of 0.45–0.80 nm. Nonlocal density functional theory (NLDFT) was used to access the pore size distribution (PSD) within the micropore size range.

Thermogravimetric analysis (TGA) was conducted by a thermogravimetric analyzer (Simultaneous Thermal Analyzer model 6000). The experiments were carried out at atmospheric pressure using N<sub>2</sub> as a purging gas (50 mL min<sup>-1</sup>) and the samples were heated from 30 to 600 °C at heating rates of 5, 10, and 15 °C min<sup>-1</sup>. The weight loss of the samples and the temperature were continuously recorded.

### 2.2 Adsorption and regeneration experiments

#### 2.2.1 Adsorption of TOL and MEK over a fixed-bed unit

Figure 1 shows the schematic diagram for the experimental setup for KBAC adsorption testing. The detailed information pertaining to VOC adsorption measurement and adsorption bed operation can be found in our previous studies [22, 24]. Briefly, the fixed-bed unit comprises a VOC generating system, a temperature-controlled fixed bed, an online total hydrocarbon (THC) analyzer (Ratfish Analysensysteme, model

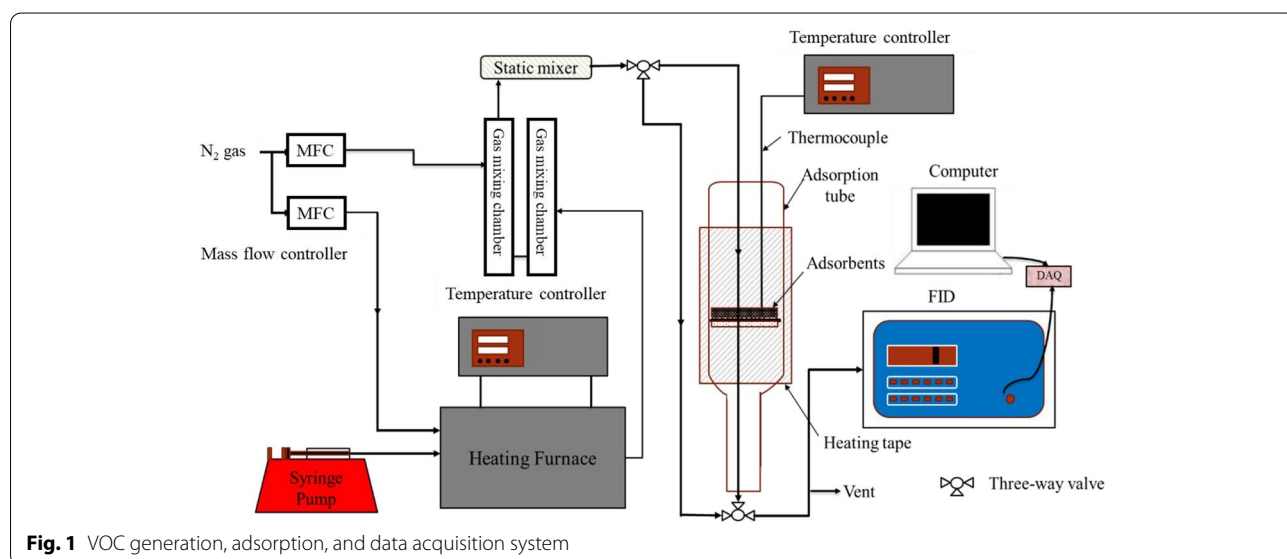


Fig. 1 VOC generation, adsorption, and data acquisition system

RS53-T), and a data acquisition (DAQ) unit consisting of a data logger (National Instruments, model USB 6000) and LabView software (National Instruments, program developed by Institute for Information Industry, Taiwan). In this study, the mixing TOL/N<sub>2</sub> or MEK/N<sub>2</sub> gas with a downward flow at 1.6 SLPM passed through a fixed-bed adsorber containing KBAC (Fig. 1). The concentration of TOL (Honeywell-Riedel-de Haën, ≥99.7%) and MEK (Merck, ≥99.0%) was controlled at 500 ppm<sub>v</sub> and the bed temperature was 30 °C. The mass of the adsorbent was 0.2 g and the corresponding height of the fixed bed was around 0.7 cm (Fig. 2). All the tests were triplicated.

Two approaches to obtain the TOL and MEK adsorption capacities are used. The first involves integrating the area above the breakthrough curve detected by the THC analyzer, while the other, directly measures the weight change before and after the adsorption/regeneration process, which, based on our preliminary tests [23, 24], demonstrated higher accuracy and consistency throughout the experiments.

For the integral method, the adsorption capacity of BAC was calculated by Eq. (1):

$$\text{Adsorption capacity} = \frac{1}{W_I} \sum_{t=0}^{t_b} Q_G (C_{in} - C_{out}) \rho_G \Delta t \quad (1)$$

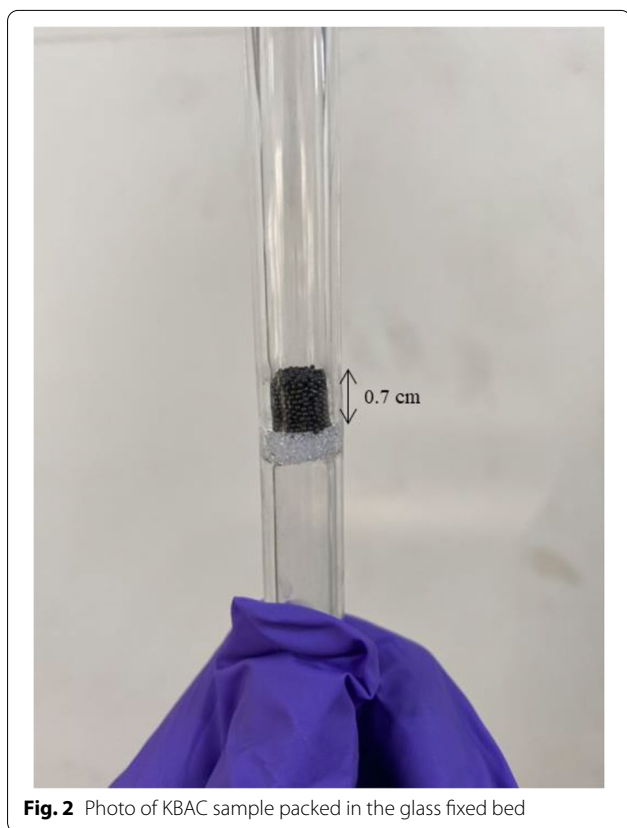


**Fig. 2** Photo of KBAC sample packed in the glass fixed bed

where  $W_I$  stands for the initial mass of dry BAC,  $Q_G$  is the total gas flow rate,  $C_{in}$  and  $C_{out}$  are the inlet and outlet concentrations during time step  $\Delta t$ , setting at 1 second in this experiment,  $\rho_G$  is the density of the organic vapor, and  $t_b$  is the time required to reach total breakthrough.

For the gravimetric method, the adsorption capacity was calculated by Eq. (2):

$$\text{Adsorption capacity} = \frac{W_{AA} - W_{BA}}{W_I} \quad (2)$$

where  $W_{AA}$  and  $W_{BA}$  indicate the weight of the adsorbent after and before the adsorption test, respectively.

### 2.2.2 ETS experiment

The ETS used for KBAC regeneration is demonstrated in Fig. 3. KBAC saturated with TOL or MEK was placed in the center of the reactor, coming into contact with two stainless steel conductive rods, which allowed the current to pass through. As the direct current (DC) and voltage were applied to the KBAC via a DC power supplier (ITECH model IT6721), the temperature of the KBAC bed increased due to the Joule effect resulting from the heterogeneously distributed conductive and resistant structures within KBAC as the current passed through. The targeted regeneration temperatures of the KBAC fixed bed, monitored by a K-type thermocouple inserted in the fixed bed and read out and controlled by a temperature controller, were set to 120, 140, and 160 °C by applying suitable power to the fixed bed ranging from 2 to 2.5 W. The applied power was manually adjusted to the target temperature and lasted for approximately 90 and 50 min for TOL and MEK desorption, respectively. The desorbed VOC outlet concentration was detected by the THC analyzer with N<sub>2</sub> as the carrier gas (1.6 SLPM). All the tests were triplicated. Desorption efficiency is described as in Eq. (3):

$$\text{Desorption efficiency (\%)} = \frac{W_{BR} - W_{AR}}{W_I \times q_{500ppmv}} \times 100\% \quad (3)$$

where  $W_{BR}$  and  $W_{AR}$  are the adsorbent's weight (mg) before and after regeneration, respectively, and  $q_{500ppmv}$  represents the adsorption capacity (mg mg<sup>-1</sup>) at 30 °C and 500 ppm<sub>v</sub>.

### 2.2.3 Cyclic adsorption and electrothermal regeneration test

The cyclic adsorption and electrothermal regeneration experiments were carried out by exposing the KBAC to TOL or MEK vapor to achieve saturation and subjected to a 6-cycle of electrothermal desorption operation. The regeneration temperatures were controlled at 120, 140, and 160 °C. The regeneration efficiency was calculated by Eq. (4):

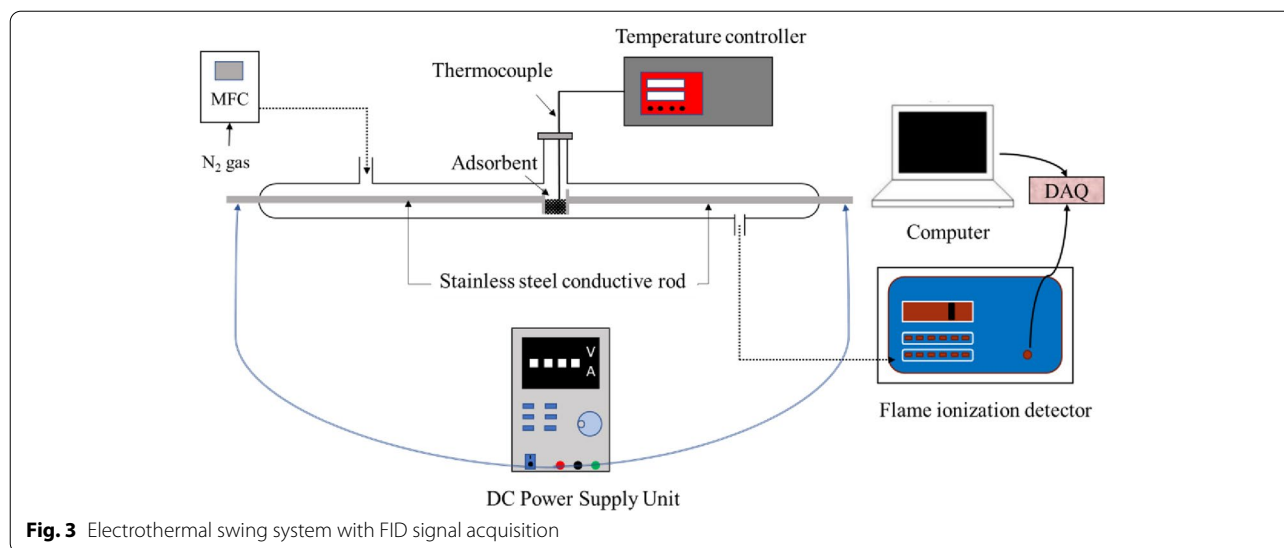


**Fig. 3** Electrothermal swing system with FID signal acquisition

$$\text{Regeneration efficiency (\%)} = \frac{q_r}{q_0} \times 100\% \quad (4)$$

where:

$q_0$  = quantity of adsorbate adsorbed per unit weight of virgin KBAC.

$q_r$  = quantity of adsorbate adsorbed per unit weight of regenerated KBAC.

### 3 Results and discussion

#### 3.1 Adsorbent characterization

##### 3.1.1 Chemical and physical properties of virgin and electrothermal regenerated KBAC

Table 1 shows the elemental analysis (EA) results for both virgin and electrothermal regenerated KBAC samples at 120, 140, and 160 °C. It is worth noting that because the EA of this study separately analyzed C/H/N/S and O, the sum of the relative contents may exceed 100%. These experimental results indicate that the carbon content decreased, while the oxygen content increased with an increase in desorption temperature. The decrease in carbon content is mainly due to hot-spot formation caused by uneven electrothermal heating [28–30], which causes the materials instantaneously heat up in limited regions, causing the vaporization of hydrocarbon species. For MEK-KBAC, however, the increase in oxygen content after electrothermal regeneration may also be attributed to the reaction of MEK with the carbon surface of KBAC. It is also worth noting that in our study, the in-situ adsorption-desorption tests could not be carried out immediately, and the increase in the oxygen content of KBAC may have been caused by the adsorption of water vapor or oxygen during placement

**Table 1** Elemental analysis results for virgin and electrothermal regenerated KBACs

Sample	C (%)	H (%)	O (%)	N (%)	S (%)
KBAC	95.6	2.59	2.96	0.44	0.47
MEK-KBAC-120 °C	92.8	2.71	4.17	0.50	0.26
MEK-KBAC-140 °C	92.8	2.98	4.96	0.60	0.22
MEK-KBAC-160 °C	85.9	2.83	9.17	0.47	0.10
TOL-KBAC-120 °C	95.6	2.41	1.70	0.26	0.00
TOL-KBAC-140 °C	95.1	2.31	2.62	0.43	0.00
TOL-KBAC-160 °C	91.5	2.13	4.87	0.31	0.00

or weighing process, which could have occurred in both TOL-KBAC and MEK-KBAC operations. Furthermore, the oxygen content presented within TOL-KBAC after the electrothermal regeneration process was lower than that of MEK-KBAC. Studies have shown that oxygen is inclined to actively interact with p-orbital electrons to exchange electrons and form chemically-bound species, resulting in less oxygen groups on the surface of TOL-KBAC, rather than MEK-KBAC after electrothermal regeneration. In other words, the lower fraction of oxygen functional groups may be due to residual chemically-adsorbed TOL on the KBAC, as the regeneration temperature was not high enough to remove 100% of adsorbed TOL [13, 24, 32, 33].

The sulfur content also decreased after desorption tests due to the chemical reaction between MEK/TOL and sulfur in BAC, where TOL was shown to be more reactive with sulfur than MEK (Table 1).

The porous properties of KBAC obtained from this study are in accordance with those previously published [34], in which  $S_{\text{total}}$  was reported as 1300 m<sup>2</sup> g<sup>-1</sup> and



$V_{micro}$  was  $0.56\text{ cm}^3\text{ g}^{-1}$ . Overall, this KBAC sample has excellent micropore development. It can be seen from Table 2 that after one adsorption/desorption cycle, the micropore area/volume of the two BAC samples was reduced, which further decreased after another 5 cycles. For micropore area, TOL-BAC decreased from 881 to  $534\text{ m}^2\text{ g}^{-1}$ , and MEK-BAC decreased from 1070 to  $694\text{ m}^2\text{ g}^{-1}$ . For micropore volume, TOL-BAC decreased from 0.36 to  $0.22\text{ cm}^3\text{ g}^{-1}$ , while MEK-BAC decreased from 0.43 to  $0.27\text{ cm}^3\text{ g}^{-1}$ . Based on these results, it can be inferred that during the cyclic adsorption and desorption process, the pores of KBAC were blocked by the coke generated from the Joule heating process, resulting in the observed decrease in pore area and volume. Importantly, with respect to pore volume ratio, the proportion of the micropores in the total volume decreased, suggesting that micropores are more affected by coke blockage than mesopores or macropores.

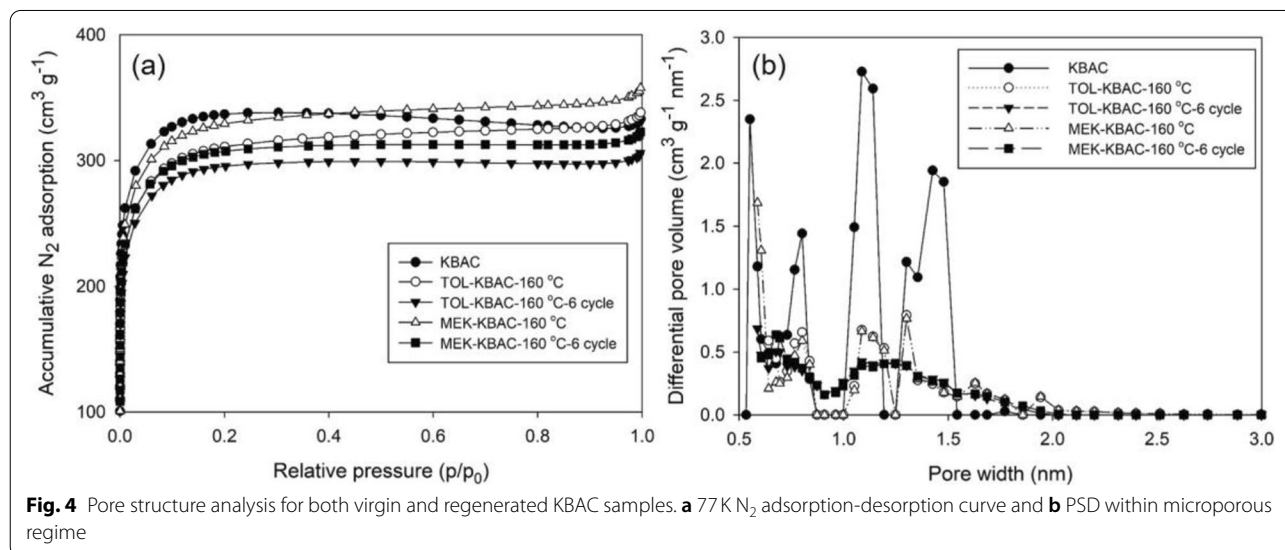
The standard  $\text{N}_2$  adsorption-desorption curves and PSD within the microporous regime for KBAC samples

are shown in Fig. 4a and b. All samples followed the Type I isotherm classified by the 2015 version of the International Union of Pure and Applied Chemistry definition, suggesting the presence of microporous structures. Notably, the  $\text{N}_2$  adsorption capacity decreased as KBAC was regenerated after saturating with TOL or MEK, and the overall trend from greatest to least follows the order: MEK-KBAC-160°C, TOL-KBAC-160°C, MEK-KBAC-160°C-6-cycle, and TOL-KBAC-160°C-6-cycle. It has been proven that TOL has a stronger affinity for AC materials due to its low- to non-polarity compared to MEK. The overall decreasing trend in  $\text{N}_2$  adsorption capacity indicated that TOL could be more challenging to desorb, and coke formation might occur during the Joule heating process, leading to the aforementioned declining trend in adsorption capacity. In addition, the TOL-KBAC-160°C-6-cycle held the smallest  $\text{N}_2$  adsorption capacity, likely due to higher amount of aggregated TOL trapped from each electrothermal regeneration procedure, which contributes to a portion of the heel

**Table 2** Surface area and pore volume analysis for KBACs

Sample	$S_{total}^a$ ( $\text{m}^2\text{ g}^{-1}$ )	$S_{micro}$ ( $\text{m}^2\text{ g}^{-1}$ )	$S_{micro}/S_{total}$ (%)	$V_{total}$ ( $\text{cm}^3\text{ g}^{-1}$ )	$V_{micro}$ ( $\text{cm}^3\text{ g}^{-1}$ )	$V_{micro}/V_{total}$ (%)
KBAC	1280	1190	93.2	0.52	0.48	91.8
MEK-KBAC-160°C	1260	1070	84.9	0.55	0.43	77.0
TOL-KBAC-160°C	1160	881	76.1	0.50	0.36	73.1
MEK-KBAC-160°C-2-cycle	1210	743	61.3	0.51	0.32	62.9
TOL-KBAC-160°C-2-cycle	1150	603	52.7	0.47	0.22	47.3
MEK-KBAC-160°C-6-cycle	1180	694	59.0	0.48	0.27	56.4
TOL-KBAC-160°C-6-cycle	1140	534	47.0	0.47	0.22	46.3

<sup>a</sup>  $S_{total}$ : specific surface area;  $S_{micro}$ : micropore surface area;  $V_{total}$ : total pore volume;  $V_{micro}$ : micropore volume



formation. Similar results can be deduced from the PSD derived using the NLDFT model for each sample, which is typically used in the pore with width less than 2 nm, with virgin KBAC possessing the highest micropore volume.

### 3.1.2 Morphology of KBAC samples

The morphology of virgin and post-regenerated KBAC under various resolutions is shown in Fig. 5. According to the micrographs, the appearance showed little difference under lower resolutions, depicting a perfectly spherical shape with a partially rough surface. Compared to virgin KBAC, the post-regenerated KBAC samples appeared to have a smoother surface, likely from the interphase reaction between VOC molecules and KBAC's surface during the electrothermal heating process or the remaining by-products after regeneration. In contrast, the corrosion phenomenon in TOL-KBAC-160°C seemed to be even more evident than in MEK-KBAC-160°C, which could be attributed to the electron transfer from the interaction between TOL molecules and oxygen functional groups on the KBAC's surface, corroding the partial surface of KBAC either during the adsorption or electrothermal regeneration processes.

### 3.1.3 TGA and differential thermal gravimetry (DTG) results

TGA and DTG can provide essential information regarding the desorption behavior of adsorbates, as well as

indicate the thermal stability of adsorbents used. In this study, the TGA analysis for virgin KBAC was carried out from room temperature to 800°C at a heating rate of 5°C min<sup>-1</sup> prior to the analysis of KBAC exposure to TOL or MEK (Fig. 6a). Significant weight loss, which could be attributed to the desorption of adsorbed water molecules in virgin KBAC, occurred between 50 and 100°C. The other sharp decrease in KBAC's weight occurred around 700–800°C, probably due to the gasification of carbonaceous species into CO or CO<sub>2</sub> (Fig. 6a). For KBAC saturated with TOL or MEK, the weight loss was observed throughout a wide range of temperatures from around 100 to 300°C, demonstrating the desorption and/or decomposition of TOL or MEK within KBAC samples (Fig. 6b and c). The TGA results of TOL/MEK saturated KBAC proved that the KBAC saturated with TOL or MEK could be successfully regenerated below 300°C.

Figure 6b and c also show that under conventional conductive heating, the weight loss percentages of loaded KBACs were less significant at rapid heating rates. This may result in more heel formation at a rapid heating rate. Niknaddaf et al. [35] indicated that increasing the heating rate or lowering the purging gas flowrate leads to higher 1,2,4-trimethylbenzene exposure at higher temperatures; therefore, residence time was extended, leading to

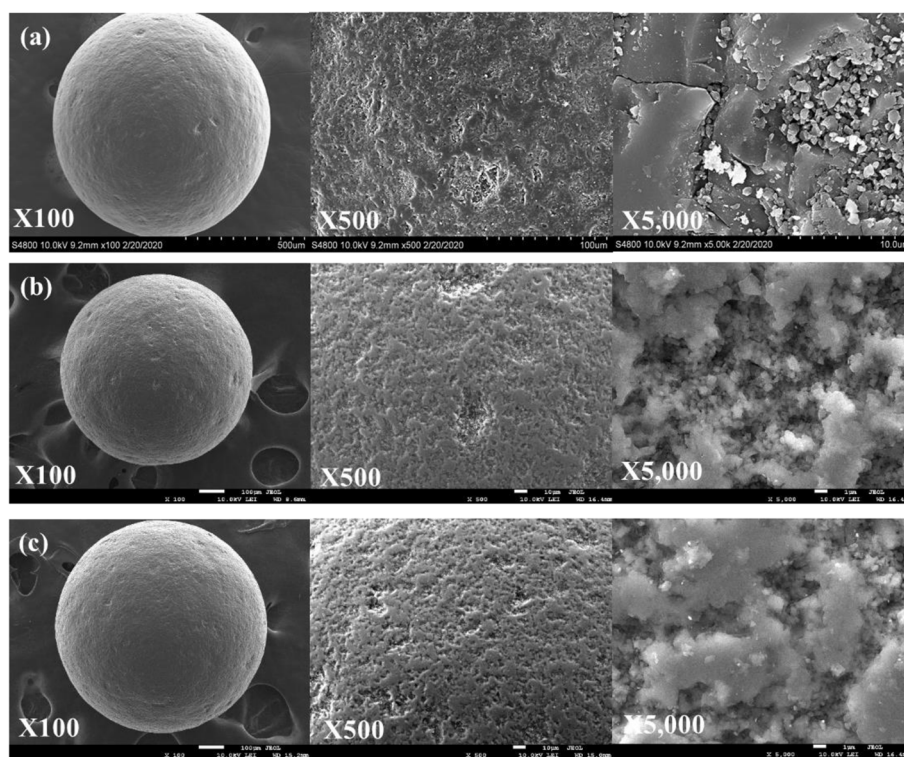


**Fig. 5** SEM micrographs of **a** virgin KBAC, **b** TOL-KBAC-160°C, and **c** MEK-KBAC-160°C under resolutions of X100, X500, and X5,000

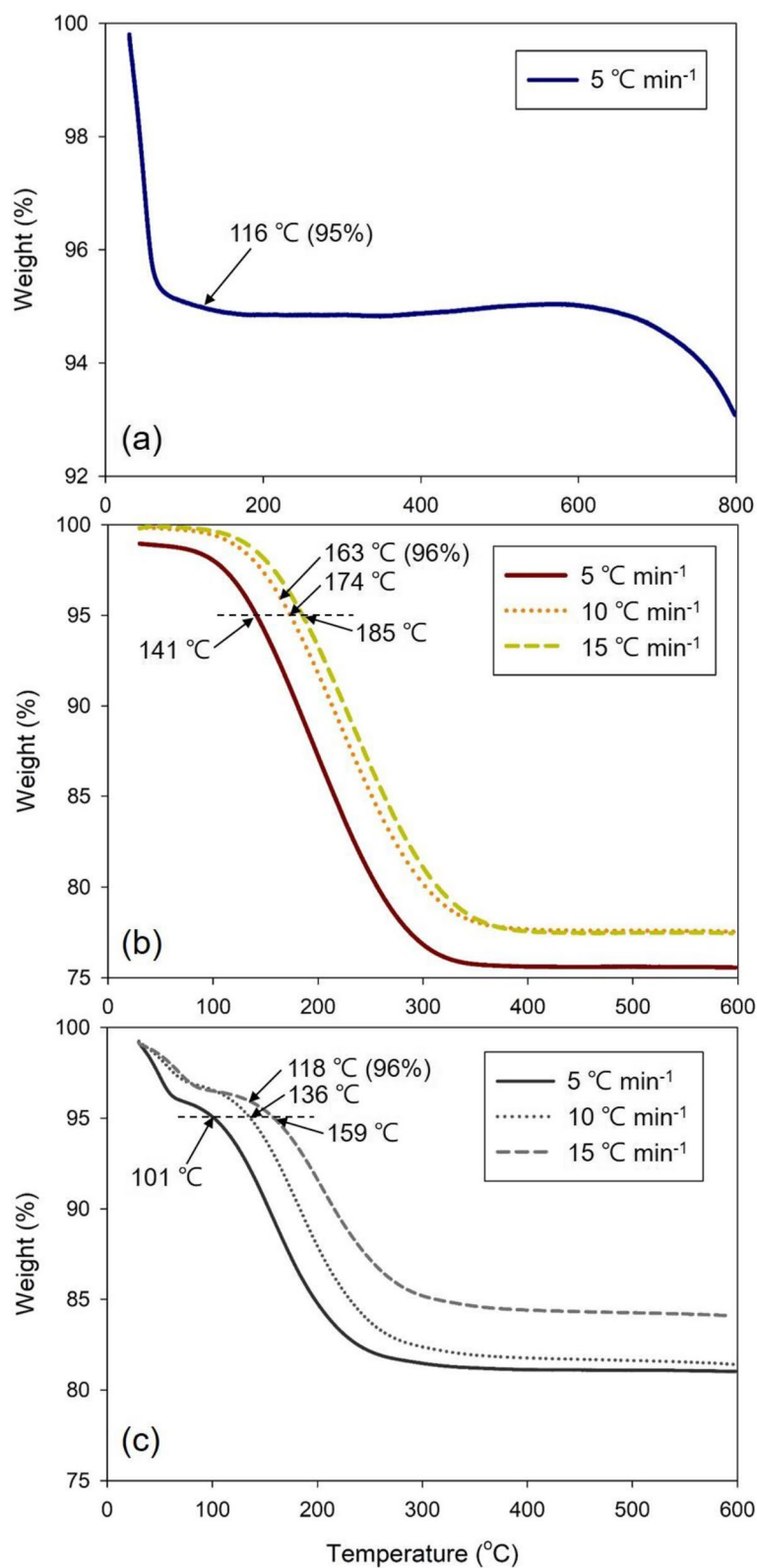


**Fig. 6** TGA desorption curves for **a** virgin KBAC at heating rate of 5 °C min<sup>-1</sup>, **b** TOL-KBAC-160 °C, and **c** MEK-KBAC-160 °C at heating rates of 5, 10, and 15 °C min<sup>-1</sup>



pore-blockage or high carbon residue (i.e., coke) within the inner structure of adsorbents. This suggests a higher chance of heel formation after regeneration.

DTG derived from TGA data was used to evaluate the activation desorption energy ( $E_d$ ) of organic compounds (Fig. 7). According to the DTG curves of TOL-KBAC and MEK-KBAC, the temperature peaks below 100 °C were attributed to water molecule desorption [36]. Since desorption temperature is highly correlated with affinity between molecule and adsorbent, a more robust interaction yields a higher desorption peak. Assuming that the desorption followed first-ordered kinetics and the heating rate was constant (i.e.,  $T = T_0 + \beta t$ ), based on the Arrhenius equation, activation desorption energy could be calculated by the following equation [37]:

$$\ln\left(\frac{\beta}{RT_M^2}\right) = \frac{E_d}{RT_M} + C \quad (5)$$

where  $T_M$  is the peak desorption temperature,  $\beta$  is the heating rate,  $E_d$  is the desorption activation energy,  $R$  is the gas constant, and  $C$  is a constant dependent on the desorption kinetics. As such, a plot of  $\ln\left(\frac{\beta}{RT_M^2}\right)$  versus  $1/T_M$  yields a straight line with a slope  $-E_d/R$ .

By using Eq. (5), the activation desorption energies of 54 and 33 kJ mol<sup>-1</sup> for TOL-KBAC and MEK-KBAC were obtained, respectively (Table 3), demonstrating that MEK was more easily desorbed from KBAC than TOL. Compared to the heat of vaporization for TOL and MEK (i.e., 32.8 and 31.2 kJ mol<sup>-1</sup> at boiling points for MEK and TOL, respectively), the calculated  $E_d$  for TOL (54 kJ mol<sup>-1</sup>) is 1.7 times larger than its corresponding heat of vaporization, yet is similar to that of MEK (33 versus 31 kJ mol<sup>-1</sup>). This result further suggests the greater affinity of TOL for KBAC than MEK, and the adsorption mechanism is dominated by physical adsorption [36]. These results are also consistent with the desorption

**Table 3** Peak desorption temperature and activation desorption energy derived from DTG for TOL-KBAC and MEK-KBAC

	Peak desorption temperature (°C)			Activation desorption energy (kJ mol <sup>-1</sup> )
	5 °C min <sup>-1</sup>	10 °C min <sup>-1</sup>	15 °C min <sup>-1</sup>	
TOL-KBAC	197	218	232	53.6
MEK-KBAC	158	182	205	33.3

efficiency obtained from the ETS desorption tests described in the following sections.

### 3.2 Electrothermal regeneration on saturated KBACs

#### 3.2.1 Shape of desorption curves and desorption efficiency

To assess the desorption performances of KBAC, the saturated samples (loaded with 500 ppm<sub>v</sub> of TOL or MEK at 30 °C) were subjected to electrothermal heating under various temperatures (120, 140, and 160 °C), at a constant N<sub>2</sub> purging flow (1.6 SLPM). The shape of the desorption curves for all the KBAC samples depicted a similar trend during the electrothermal heating process (Fig. 8). In addition to the peak concentrations with varying input power during the process, the desorption curves occurred later at lower regeneration temperatures (i.e., 120 and 140 °C), likely resulting from the nonhomogeneous heat transfer among the fixed bed of KBAC samples. The highest concentration for TOL and MEK peaked at around 600 and 1000 ppm<sub>v</sub> at 160 °C, further demonstrating that TOL was more challenging to desorb and would likely form more coke to block the pore structures.

The desorption efficiency shown in Fig. 9 was evaluated by both gravimetric and integral methods. The gravimetric method involved weighing adsorbents before and after the electrothermal regeneration, while the integral approach integrated the area beneath the desorption curves recorded by the FID. Generally, the desorption

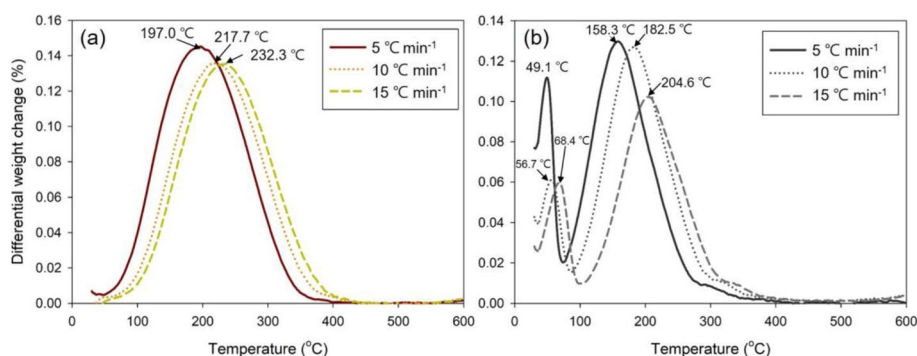
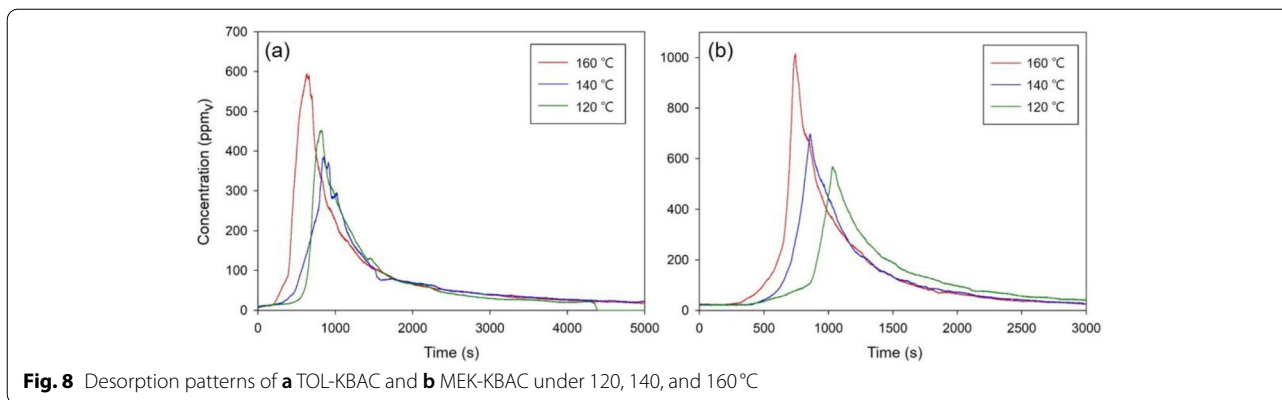


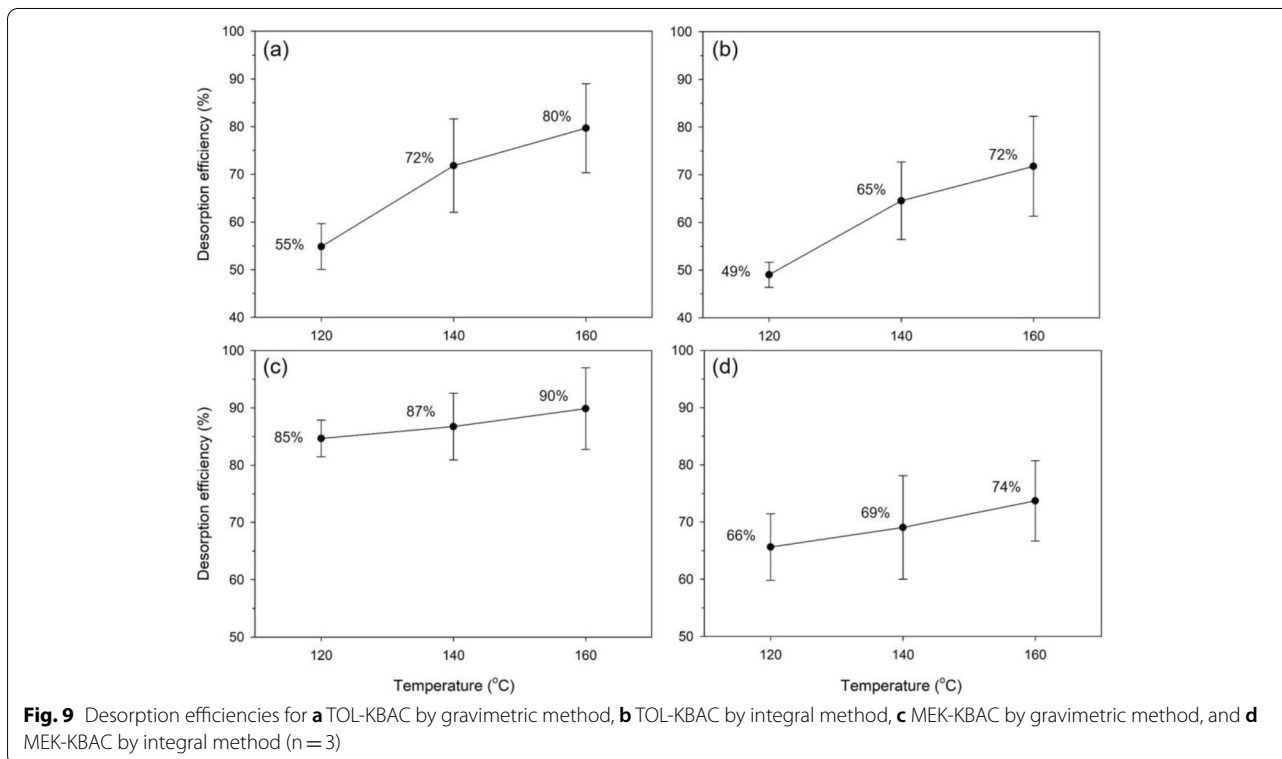
**Fig. 7** DTG curves for **a** TOL-KBAC and **b** MEK-KBAC under heating rates of 5, 10, and 15 °C min<sup>-1</sup>



efficiency for TOL-KBAC and MEK-KBAC obtained by measuring the weight change ranged from 55 to 80% and 85 to 90%, respectively, whereas, the calculated desorption efficiency by integral method was consistently lower for both TOL-KBAC and MEK-KBAC, ranging from 49 to 72% and 66 to 74%, respectively.

The desorption efficiency for MEK-KBAC was higher than TOL-KBAC, either estimated by the gravimetric or integral method, which could be attributed to the lower boiling point of MEK and greater affinity of TOL for KBAC, as shown in the TGA/DTG analytical results. For TOL-KBAC, the efficiency evaluated by desorption

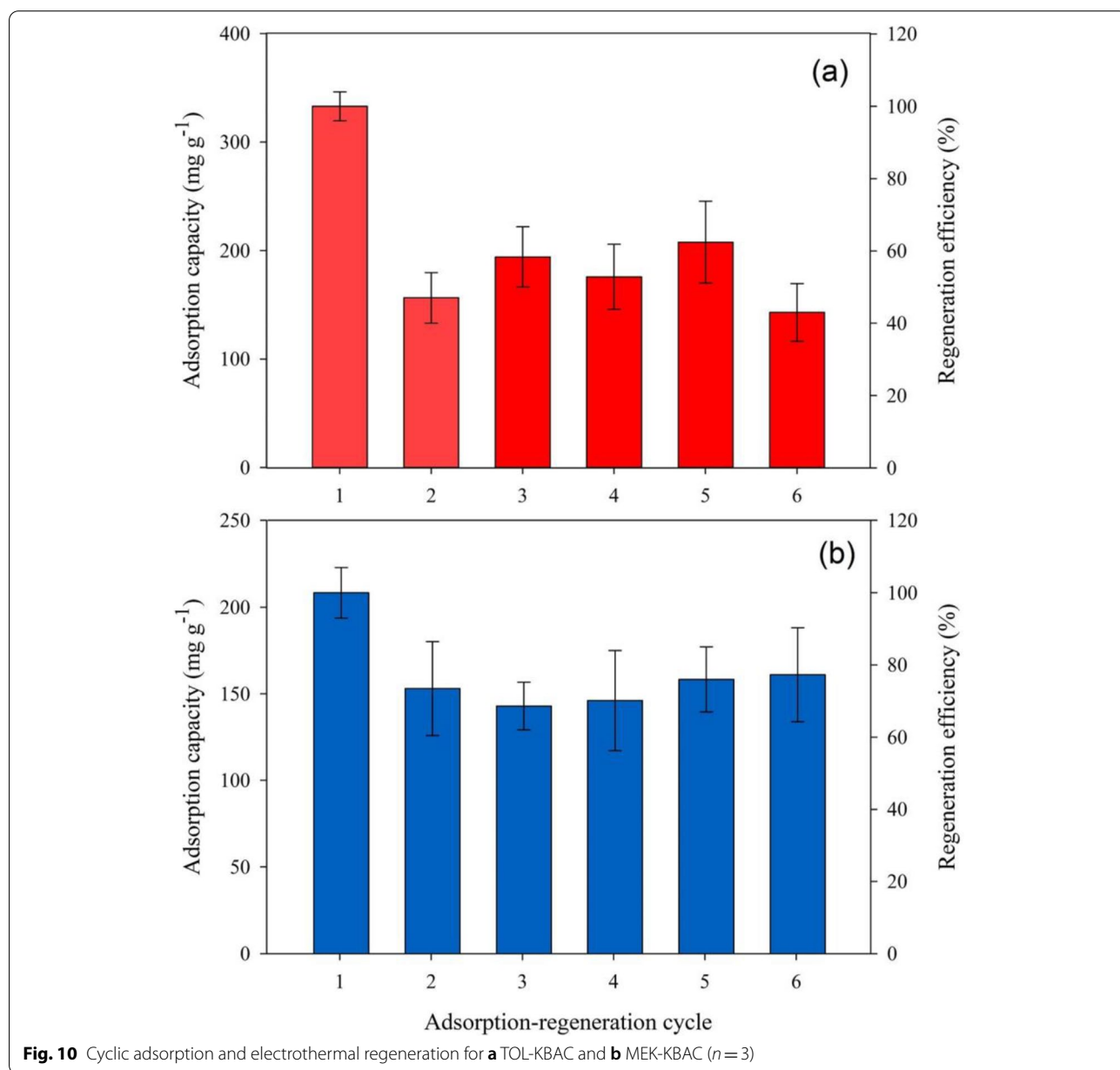
concentration was slightly lower than that by weight change (−7% on the average for TOL-KBAC at three desorption temperatures). However, for MEK-KBAC, the desorption efficiency calculated from the mass balance of the desorption concentration was significantly lower than that calculated from weight change (−18% on the average for MEK-KBAC under three desorption temperatures). These results are inconsistent with our previous study [24], whose measured efficiency via gravimetric method was consistently more notable than that of the integral approach. These results may be due to the decomposition of organic compounds or the release of



impurities that were undetected by THC analyzer [5]. Hsiao et al. [24] employed a gas analyzer downstream of the microwave regeneration system to measure the composition of the tail gas stream. For MEK-KBAC, the decomposition of MEK into CO or CO<sub>2</sub> could not be measured by the THC analyzer [38], furthering the inconsistency in desorption efficiency of MEK-KBAC as evaluated by gravimetric and integral methods. In contrast, significant SO<sub>2</sub> emission (25.04 μg as S) during the regeneration process occurred from sulfur removal at higher temperatures, leading to a possible overestimation of desorption efficiency by the gravimetric method.

### 3.2.2 Cyclic electrothermal swing adsorption and regeneration experiments

Figure 10 shows the saturated adsorption capacity and the regeneration efficiency of TOL-KBAC's and MEK-KBAC's 6-cycle electrothermal operation under 160 °C. We defined the regeneration efficiency as the comparison between the adsorption capacities of the regenerated versus virgin KBAC. According to the results, the regeneration efficiency for TOL-KBAC drastically reduced from 100 to around 50–60% compared with 70–80% for MEK-KBAC, inferring that possible pore blockage due to coke formation or heel buildup during the electrothermal



heating process is more severe in TOL adsorption. It is also worth noting that the adsorption capacity for regenerated TOL-KBAC, though reduced to 50% of initial capacity, fluctuating between 160 and 210 mg g<sup>-1</sup>, still proved higher than that of MEK-KBAC, which could be due to stronger affinity toward low to nonpolar aromatic hydrocarbons such as TOL.

Comparing the ETS regeneration results with our previous work [24] using microwave regeneration at 800–1000 W power, the regeneration efficiency for TOL-KBAC and MEK-KBAC was both approximately 75–100%, indicating that microwaves effectively provide energy to heat saturated KBAC. Direct heating regeneration induced from electrothermal Joule effects seems to cause adverse effects in pore structures, which is of great concerns when used in future real-scale application.

Importantly, the ETS regeneration efficiency for MEK decreased slightly to approximately 80% and remained stable throughout the 6-cycle electrothermal adsorption/regeneration. The relatively higher ratio of regeneration efficiency of MEK-KBAC noted advanced potential in MEK recovery by regenerable adsorbents either in lab- or engineering-scale industries. Meanwhile, the cyclic electrothermal adsorption and regeneration experiments provided a novel technique in VOC recovery via the more effective and energy-efficient electrothermal heating with greater prospects.

#### 4 Conclusions

The present study reported a successful application of a novel and promising electrothermal regeneration technique in cyclic VOCs adsorption and desorption on a commercially available BAC (i.e., KBAC) toward TOL and MEK. The physical and chemical analyses showed that KBAC possessed an ultra-high surface area and pore volume with well-developed microporous structures favorable for VOC capture via physisorption. The N<sub>2</sub> adsorption analysis revealed that the decrease in surface area and pore volume of KBAC may result from pore structure collapse or pore blockage due to coke formation. The peak desorption temperature as well as the desorption activation energy proved that the affinity between TOL and the KBAC surface was stronger than that of MEK. The desorption efficiency for TOL-KBAC was consistently lower than MEK-KBAC, serving as more evidence that MEK is easier to recover either in a lab- or engineering-scale site compared to TOL. In addition, the difference in the desorption efficiency using the gravimetric method and the integral method was likely due to the decomposition of adsorbates into CO, CO<sub>2</sub>, or sulfur dioxide (SO<sub>2</sub>). Finally, the decrease in the regeneration efficiency from 100% to 50–60% for TOL-KBAC was more significant than for MEK-KBAC, suggesting that formation of coke blocks the pores and causes heel buildup during desorption.

The novelty and rationality of this study are that we have proven the feasibility of using an electrothermal swing system in adsorbent regeneration to be more energy-efficient without wastewater or byproduct generation as compared to conventional steam regeneration. However, future research should focus on how to control the power supply and track the adsorbent bed's temperature accurately to further improve efficiency and accuracy in electrothermal regeneration on adsorbents.

#### Acknowledgements

This work was financially supported by the Ministry of Science and Technology, Taiwan under Grant no. 108-2218-E-002-068-MY3. The opinions expressed in this paper are not necessarily those of the sponsor.

#### Authors' contributions

Conceptualization, H.C.H., C.W., and J.G.D.; methodology, H.C.Y. and H.C.H.; formal analysis, H.C.Y. and S.W.Y.; data curation, H.C.Y. and S.W.Y.; writing—original draft preparation, H.C.Y. and H.C.H.; writing—review and editing, S.W.Y. and H.C.H.; visualization, H.C.Y.; funding acquisition, H.C.H., C.W., and J.G.D. All authors read and approved the final manuscript.

#### Funding

This work was financially supported by the Ministry of Science and Technology, Taiwan under Grant no. 108-2218-E-002-068-MY3. The opinions expressed in this paper are not necessarily those of the sponsor.

#### Availability of data and materials

All data generated or analyzed during this study are included in this published article.

#### Declarations

#### Competing interests

The authors declare they have no competing interests.

#### Author details

<sup>1</sup>Graduate Institute of Environmental Engineering, National Taiwan University, Taipei 10617, Taiwan. <sup>2</sup>School of Environmental Science and Engineering, Tianjin University, Tianjin 300072, China. <sup>3</sup>Tianjin Key Lab of Indoor Air Environmental Quality Control, Tianjin 300072, China. <sup>4</sup>College of Environmental and Energy Engineering, Beijing University of Technology, Beijing 100124, China.

Received: 11 September 2022 Accepted: 10 December 2022

Published online: 28 December 2022

#### References

- Zhang XY, Gao B, Creamer AE, Cao CC, Li YC. Adsorption of VOCs onto engineered carbon materials: a review. *J Hazard Mater*. 2017;338:102–23.
- Huang YS, Hsieh CC. VOC characteristics and sources at nine photochemical assessment monitoring stations in western Taiwan. *Atmos Environ*. 2020;240:117741.
- Gu S, Guenther A, Faiola C. Effects of Anthropogenic and biogenic volatile organic compounds on Los Angeles air quality. *Environ Sci Technol*. 2021;55:12191–201.
- Hanif NM, Hawari NSSL, Othman M, Abd Hamid HH, Ahamad F, Uning R, et al. Ambient volatile organic compounds in tropical environments: potential sources, composition and impacts – a review. *Chemosphere*. 2021;285:131355.
- Kim KJ, Ahn HG. The effect of pore structure of zeolite on the adsorption of VOCs and their desorption properties by microwave heating. *Micropor Mesopor Mat*. 2012;152:78–83.
- Le Cloirec P. Adsorption onto activated carbon fiber cloth and electrothermal desorption of volatile organic compound (VOCs): a specific review. *Chinese J Chem Eng*. 2012;20:461–8.



7. Sui H, Liu HX, An P, He L, Li XG, Cong S. Application of silica gel in removing high concentrations toluene vapor by adsorption and desorption process. *J Taiwan Inst Chem E*. 2017;74:218–24.
8. Ghafari M, Atkinson JD. Impact of styrenic polymer one-step hyper-cross-linking on volatile organic compound adsorption and desorption performance. *J Hazard Mater*. 2018;351:117–23.
9. Xu C, Ruan CQ, Li YX, Lindh J, Stromme M. High-performance activated carbons synthesized from nanocellulose for CO<sub>2</sub> capture and extremely selective removal of volatile organic compounds. *Adv Sustain Syst*. 2018;2:1700147.
10. Lv YT, Sun J, Yu GQ, Wang WL, Song ZL, Zhao XQ, et al. Hydrophobic design of adsorbent for VOC removal in humid environment and quick regeneration by microwave. *Micropor Mesopor Mat*. 2020;294:109869.
11. Zhang HH, Dai LY, Feng Y, Xu YH, Liu YX, Guo GS, et al. A Resource utilization method for volatile organic compounds emission from the semiconductor industry: selective catalytic oxidation of isopropanol to acetone over Au/ $\alpha$ -Fe<sub>2</sub>O<sub>3</sub> nanosheets. *Appl Catal B-Environ*. 2020;275:119011.
12. Wickramaratne NP, Jaroniec M. Importance of small micropores in CO<sub>2</sub> capture by phenolic resin-based activated carbon spheres. *J Mater Chem A*. 2013;1:112–6.
13. Zhang GZ, Lei BM, Chen SM, Xie HM, Zhou GL. Activated carbon adsorbents with micro-mesoporous structure derived from waste biomass by stepwise activation for toluene removal from air. *J Environ Chem Eng*. 2021;9:105387.
14. Li YD, Shen YH, Niu ZY, Tian JP, Zhang DH, Tang ZL, et al. Process analysis of temperature swing adsorption and temperature vacuum swing adsorption in VOCs recovery from activated carbon. *Chinese J Chem Eng*. 2022; In press. <https://doi.org/10.1016/j.cjche.2022.01.029>.
15. Zhu ZL, Li AM, Zhong S, Liu FQ, Zhang QX. Preparation and characterization of polymer-based spherical activated carbons with tailored pore structure. *J Appl Polym Sci*. 2008;109:1692–8.
16. Qian QL, Gong CH, Zhang ZG, Yuan GQ. Removal of VOCs by activated carbon microspheres derived from polymer: a comparative study. *Adsorption*. 2015;21:333–41.
17. Wang Q, Liang XY, Qiao WM, Liu CJ, Liu XJ, Zhan LA, et al. Preparation of polystyrene-based activated carbon spheres with high surface area and their adsorption to dibenzothiophene. *Fuel Process Technol*. 2009;90:381–7.
18. Qi JW, Li JS, Li Y, Fang XF, Sun XY, Shen JY, et al. Synthesis of porous carbon beads with controllable pore structure for volatile organic compounds removal. *Chem Eng J*. 2017;307:989–98.
19. Zhang CM, Song W, Zhang XC, Li R, Zhao SJ, Fan CM. Synthesis, characterization and evaluation of resin-based carbon spheres modified by oxygen functional groups for gaseous elemental mercury capture. *J Mater Sci*. 2018;53:9429–48.
20. Luo L, Ramirez D, Rood MJ, Grevillot G, Hay KJ, Thurston DL. Adsorption and electrothermal desorption of organic vapors using activated carbon adsorbents with novel morphologies. *Carbon*. 2006;44:2715–23.
21. Romero-Anaya AJ, Lillo-Rodenas MA, Linares-Solano A. Spherical activated carbons for low concentration toluene adsorption. *Carbon*. 2010;48:2625–33.
22. Chen YT, Huang YP, Hsi HC. Valorizing waste bamboo tar to novel bead carbonaceous adsorbent for volatile organic compound removal. *J Environ Eng*. 2019;145:04019088.
23. Chen YT, Huang YP, Wang C, Deng JG, Hsi HC. Comprehending adsorption of methylethylketone and toluene and microwave regeneration effectiveness for beaded activated carbon derived from recycled waste bamboo tar. *J Air Waste Manage*. 2020;70:616–28.
24. Hsiao SY, You SW, Wang C, Deng JG, Hsi HC. Adsorption of volatile organic compounds and microwave regeneration on self-prepared high-surface-area beaded activated carbon. *Aerosol Air Qual Res*. 2022;22:220010.
25. Sullivan PD, Rood MJ, Grevillot G, Wander JD, Hay KJ. Activated carbon fiber cloth electrothermal swing adsorption system. *Environ Sci Technol*. 2004;38:4865–77.
26. Mallouk KE, Rood MJ. Performance of an electrothermal swing adsorption system with postdesorption liquefaction for organic gas capture and recovery. *Environ Sci Technol*. 2013;47:7373–9.
27. Zhao QH, Wu F, He YDA, Xiao P, Webley PA. Impact of operating parameters on CO<sub>2</sub> capture using carbon monolith by Electrical Swing Adsorption technology (ESA). *Chem Eng J*. 2017;327:441–53.
28. Chen BC, Tsai CY, Pan SY, Chen YT, Hsi HC. Sustainable recovery of gaseous mercury by adsorption and electrothermal desorption using activated carbon fiber cloth. *Environ Sci Technol*. 2020;54:1857–66.
29. Liao HY, Pan SY, You SW, Hou CH, Wang C, Deng JG, et al. Mercury vapor adsorption and sustainable recovery using novel electrothermal swing system with gold-electrodeposited activated carbon fiber cloth. *J Hazard Mater*. 2021;410:124586.
30. You SW, Liao HY, Tsai CY, Wang C, Deng JG, Hsi HC. Using novel gold nanoparticles-deposited activated carbon fiber cloth for continuous gaseous mercury recovery by electrothermal swing system. *Chem Eng J*. 2022;431:134325.
31. Zhao RK, Liu LC, Zhao L, Deng S, Li HL. Thermodynamic analysis on carbon dioxide capture by Electric Swing Adsorption (ESA) technology. *J CO<sub>2</sub> Util*. 2018;26:388–96.
32. Yang CT, Miao G, Pi YH, Xia QB, Wu JL, Li Z, et al. Abatement of various types of VOCs by adsorption/catalytic oxidation: a review. *Chem Eng J*. 2019;370:1128–53.
33. Wang HY, Xie HM, Cao QH, Li XL, Liu BY, Gan ZX, et al. Hierarchical porous activated carbon from waste *Zanthoxylum bungeanum* branches by modified H<sub>3</sub>PO<sub>4</sub> activation for toluene removal in air. *Environ Sci Pollut R*. 2022;29:35443–58.
34. Zhu WD, Groen JC, Kapteijn F, Moulijn JA. Adsorption of butane isomers and SF<sub>6</sub> on Kureha activated carbon: 1 Equilibrium. *Langmuir*. 2004;20:5277–84.
35. Niknaddaf S, Atkinson JD, Gholidoust A, Fayaz M, Awad R, Hashisho Z, et al. Influence of purge gas flow and heating rates on volatile organic compound decomposition during regeneration of an activated carbon fiber cloth. *Ind Eng Chem Res*. 2020;59:3521–30.
36. Popescu M, Joly JP, Carre J, Danatou C. Dynamical adsorption and temperature-programmed desorption of VOCs (toluene, butyl acetate and butanol) on activated carbons. *Carbon*. 2003;41:739–48.
37. Cvetanovic RJ, Amenomiya Y. Temperature programmed desorption technique for investigation of practical catalysts. *Cataly Rev*. 1972;6:21–48.
38. Bhandari PN, Kumar A, Bellmer DD, Huhnke RL. Synthesis and evaluation of biochar-derived catalysts for removal of toluene (model tar) from biomass-generated producer gas. *Renew Energ*. 2014;66:346–53.

## Publisher's Note

Springer Nature remains neutral with regard to jurisdictional claims in published maps and institutional affiliations.

Ready to submit your research? Choose BMC and benefit from:

- fast, convenient online submission
- thorough peer review by experienced researchers in your field
- rapid publication on acceptance
- support for research data, including large and complex data types
- gold Open Access which fosters wider collaboration and increased citations
- maximum visibility for your research: over 100M website views per year

At BMC, research is always in progress.

Learn more [biomedcentral.com/submissions](https://biomedcentral.com/submissions)

